International Journal of Nanomedicine

Dovepress
open access to scientific and medical research

Open Access Full Text Article

ORIGINAL RESEARCH

Magnetic multiwalled carbon nanotubes with controlled release of epirubicin: an intravesical instillation system for bladder cancer

This article was published in the following Dove Medical Press journal:
International Journal of Nanomedicine

Ning Suo[1]
Muwen Wang[1]
Yang Jin[1]
Jun Ding[2]
Xueping Gao[3]
Xiaoliang Sun[1]
Haiyang Zhang[1]
Meng Cui[4]
Jilu Zheng[1]
Nianlu Li[5]
Xunbo Jin[1,*]
Shaobo Jiang[1,*]

[1]Department of Urology, Shandong Provincial Hospital Affiliated to Shandong University, Jinan 250021, China; [2]Department of Mechanical Engineering, University of Maryland, Baltimore County, Baltimore, MD, 21250, USA; [3]School of Material Science and Engineering, Shandong University, Jinan 250100, China; [4]Department of Urology, Shandong Provincial Maternity and Childcare Hospital, Jinan 250014, China; [5]School of Chemistry and Chemical Engineering, Shandong University, Jinan 250100, China

*These authors contributed equally to this work

Correspondence: Xunbo Jin; Shaobo Jiang
Department of Urology, Shandong Provincial Hospital Affiliated to Shandong University, Jinan, Shandong 250021, China
Tel +86 151 6888 6899;
+86 135 7377 8407
Fax +86 531 6877 7697
Email jxb@sdu.edu.cn;
jiangshaobo@sdu.edu.cn

Background: Traditional intravesical instillation treatment in bladder cancer has limited efficacy, which results in a high frequency of recurrence.

Purpose: The aim of this study was to report on an epirubicin (EPI)-loaded magnetic multiwalled carbon nanotube (mMWCNTs-EPI) system for intravesical instillation in place of the current formulation.

Methods: The mMWCNTs-EPI system was formulated with carboxylated MWCNTs, Fe_3O_4 magnetic nanoparticles, and EPI. Features and antitumor activity of the system were investigated.

Results: Under the effect of external magnets, the mMWCNTs-EPI system showed sustained release and prolonged retention behavior and better antitumor activity than free EPI. The mMWCNTs-EPI system had higher efficiency in enhancing cytotoxicity and inhibiting proliferation in vitro and in vivo than free EPI. Our studies also revealed the atoxic nature of mMWCNTs.

Conclusion: These findings suggested that mMWCNTs are effective intravesical instillation agents with great potential for clinical application.

Keywords: carbon nanotubes, intravesical instillation, epirubicin, intravesical drug delivery

Introduction

Urothelial bladder cancer (UBC) is a common malignancy with significant impact on public health. Approximately 75% of newly diagnosed UBCs are non-muscle-invasive BC (NMIBC).[1] After transurethral resection of bladder tumors, up to 70% of NMIBC patients experience disease recurrence.[2,3] NMIBC has the highest recurrence rate among solid tumors[4] and is the most expensive cancer over the lifetime of the patient, due to its high frequency of recurrence.[5,6]

NMIBC recurs because of topical occult micrometastases in bladder.[7] The conventional systemic administration of drugs is ineffective in bladder diseases, due to poorly vascularized urothelium. As such, intravesical instillation has been used, whereby a drug is directly instilled into the bladder via a catheter to attain high local concentrations with minimal systemic effects.[8] The limitations of traditional intravesical instillation are primarily due to insufficient perfusion and limited retention of the chemotherapy drugs in bladders with periodical urination. Therefore, new strategies for improving intravesical instillation therapy are an important research topic.

Magnetic nanoparticles (NPs) with good superparamagnetic behavior have attracted much attention, due to their inherent material properties and huge potential in cancer diagnosis[9–11] and treatment.[12] Our previous studies have demonstrated that

submit your manuscript | www.dovepress.com
Dovepress
http://dx.doi.org/10.2147/IJN.S189688

thermosensitive hydrogel systems including Fe_3O_4 magnetic NPs prolonged the retention of chemotherapy drugs in bladders with external magnets.[13,14] However, these systems have limited impact on disease sites. First, most drugs in hydrogel systems would separate from bladder mucosa via the loose structure of the cross-linking. Second, the hydrogel may swell and block the vesicoureteric junction. Third, temperature-dependent preparation of hydrogel systems would restrict clinical applications.

We describe a novel magnetic carboxylated multiwalled carbon nanotube (mMWCNTs)-based system with nanoscale characteristics that solves these issues. CNTs have a large surface area and are conjugated easily to chemotherapy drugs,[15] including single-walled CNTs[16] or MWCNTs.[17] MWCNTs have lower biological toxicity than single-walled CNTs.[18] Strong acid-carboxylated MWCNTs (MWCNTs-COOH) not only mitigate toxicity[19] but also increase the dispersibility and efficiency of loaded drugs.[20]

For patients with NMIBC, early intravesical instillation with epirubicin (EPI) after transurethral resection of bladder tumors is an effective method. MWCNTs–COOH can efficiently load EPI via supramolecular π–π stacking because of a large surface area and hydrogen bonding.[20] Therefore, we propose an mMWCNTs-based delivery system for intravesical EPI instillation with external magnets. This scheme is flexible, because the magnet controls drug delivery.

Methods

Materials

MWCNTs (diameter 20–50 nm, length 10–30 μm, purity >95%) were purchased from Nanotech Port (Shenzhen, China). Reagents were acquired: sulfuric acid, nitric acid, ammonium hydroxide, $FeCl_2{\cdot}4H_2O$, and $FeCl_3{\cdot}6H_2O$ (Analytical Reagent) from Sinopharm Chemical Reagent (Shanghai, China); antibodies to BCL2, BAX, and Ki67 from Abcam (Cambridge, UK); antibody to cleaved caspase 3 from Cell Signaling Technology (Danvers, MA, USA); EPI from Selleck Chemicals (Houston, TX, USA); a fluorescein isothiocyanate (FITC)–annexin V apoptosis-detection kit from BD Biosciences (San Jose, CA, USA); *N*-methyl-*N*-nitrosourea (MNU), DAPI, and FITC-labeled phalloidin from Sigma-Aldrich (St Louis, MO, USA); CCK8 from Dojindo Laboratories (Kumamoto, Japan); and a Cell Light ethynyl deoxyuridine (EdU) Apollo 567 in vitro imaging kit from RiboBio (Guangzhou, China). The human bladder transitional-cell carcinoma 5637 and T24 cell lines were kindly provided by the Stem Cell Bank, Chinese Academy of Sciences in 2016. Eight-week-old female Wistar rats were obtained from the Experimental Animal Center of Shandong University. Animal care and protocols were approved by the Institutional Animal Care and Use Committee of Shandong University. All animal experiments were performed in adherence with the National Institutes of Health *Guide for the Care and Use of Laboratory Animals*.

Preparation of mMWCNTs

mMWCNTs preparation is illustrated in Scheme 1A. Fe_3O_4 were attached to a chemically modified MWCNTs–COOH surface, producing mMWCNTs. First, 750 mg MWCNTs were dispersed in 300 mL solution of mixed acid (sulfuric acid:nitric acid 1:3) by 80 kHz sonication with a KQ-500DE digital-control ultrasonic cleaner (Kunshan Ultrasonic Instruments) for 30 minutes and then heated to 95°C for 4 hours. The MWCNTs were transformed into MWCNTs–COOH

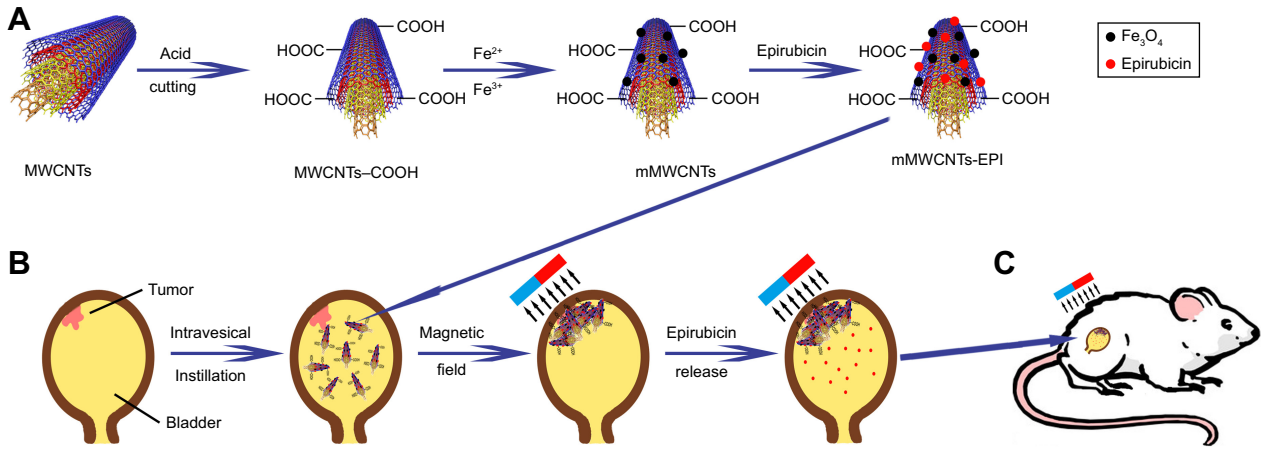

Scheme 1 Schematic illustrations of preparation and use of mMWCNTs-EPI system.
Notes: (**A**) Synthesis of mMWCNTs; (**B**) release of EPI from system; (**C**) application of the system in rats.
Abbreviations: MWCNTs, multiwalled carbon nanotubes; MWCNTs-COOH, carboxylated MWCNTs; mMWCNTs, magnetic MWCNTs-COOH; EPI, epirubicin.

with mixed-acid treatment. The MWCNTs–COOH were subsequently dried in a drying oven. Next, 100 mg dried MWCNTs–COOH were dispersed in double-distilled water, and then 42.8 mg $FeCl_2 \cdot 4H_2O$ and 116.8 mg $FeCl_3 \cdot 6H_2O$ were added (the feed molar ratio of Fe^{2+}:Fe^{3+} was 1:2). The weight ratio of MWCNTs–COOH to Fe_3O_4 was 2:1. After sonication for 5 minutes, the solution was purged with Ar_2 for 30 minutes. The reaction system was then heated to 60°C and ammonium hydroxide added. The reaction system was kept at 60°C for 2 hours and then 90°C for 30 minutes. Finally, the resulting mMWCNTs were washed six times with 200 mL double-distilled water and dried in an oven. The dried mMWCNTs were laid out thinly on an ultraclean stage (Bolante Laboratory System Engineering, Suzhou, China) and bacteria/spore-free mMWCNTs produced by ultraviolet radiation for 6 hours.[21]

Characterization of mMWCNTs

Transmission electron-microscopy images were obtained with a JEM-1011 (JEOL, Tokyo, Japan). Field-emission scanning electron-microscopy images were obtained with an SU-70 system (Hitachi, Tokyo, Japan). The ζ-potential measurements of the mMWCNTs were confirmed with a Delsa Nano C particle analyzer (Beckman Coulter, Brea, CA, USA). Fourier-transform infrared spectroscopy (FTIR) spectra were determined on an Alpha FTIR spectrometer (Bruker, Billerica, MA, USA). The crystalline structure of mMWCNTs was determined by powder diffractometry (X'Pert^3; Panalytical, Almelo, Netherlands). Magnetization evaluation was carried out with a MicroMag 2900 AGM (Lake Shore Cryotronics, Westerville, OH, USA) according to the manufacturer's instruction at room temperature.

Cell culture

T24 cells were grown in McCoy's 5A medium supplemented with 10% FBS, and 5637 cells were grown in RPMI 1640 medium supplemented with 10% FBS. All cells were grown at 37°C in an atmosphere containing 5% CO_2 and 95% air.

Cell-viability assays

The cytotoxicity of mMWCNTs was evaluated with CCK8 assays. T24 and 5637 cells were seeded onto 96-well plates at a density of 5×10^3 cells/well. After attaching to the surface of a plate, cells were treated with 0, 0.625, 1.25, 2.5, 5, 10, 20, and 40 μg/mL mMWCNTs for 72 hours. Cells were subsequently treated with CCK8 solution and incubated for an additional 4 hours. Optical density was measured using an absorbance microplate reader (Thermo Fisher Scientific, Waltham, MA, USA).

CCK8 assays were also performed to test the antitumor activity of mMWCNTs-EPI against 5637 and T24 cells. Group 1 was the control. Groups 2–4 were treated for 24 hours with a magnetic field and 40 μg/mL mMWCNTs; 2 μg/mL EPI; and a magnetic field and mMWCNTs-EPI (containing 2 μg/mL EPI), respectively. The culture medium was refreshed at 2, 4, 6, 8, 10, 12, and 24 hours to mimic urination. CCK8 solution was added in accordance with the aforementioned protocol.

Cell-morphology tests

T24 and 5637 cells were divided into control groups and experimental groups, respectively. Experimental groups were treated with 40 μg/mL mMWCNTs for 72 hours. Control groups were treated with PBS for the same time. Cells were fixed with methanol for 10 minutes and stained with FITC-labeled phalloidin for 1 hour. Nuclei were counterstained with DAPI. Images were captured using fluorescence microscopy (Olympus, Tokyo, Japan).

In vivo toxicity of mMWCNTs

The toxicity of mMWCNTs in vivo was determined in 12 female rats. Six rats were maintained in the magnetic field with 3,200 G magnets fixed near their bladders. Then, 2.5 mg/1 mL mMWCNTs were instilled intravesically every 3 days for 1 month. Another six rats were fed as controls. Blood samples were collected after 1 month for analysis of blood serum chemistry. ALT, AST, Scr, and BUN were determined with a fully automatic biochemical analyzer (Chemray 240; Rayto Life and Analytical Sciences, Shenzhen, China). Hearts, livers, spleens, lungs, kidneys, and brains were excised at the same time to detect the systemic toxicity of mMWCNTs.

Loading and release studies

EPI was dissolved in double-distilled water at a concentration of 1 mg/mL. The same mass of mMWCNTs was then mixed into EPI solution by sonication for 30 minutes. mMWCNTs-EPI were produced and then purified via external magnets. Briefly, the suspension of mMWCNTs-EPI and free EPI was placed on a magnetic rack (Solarbio Life Sciences, Beijing, China) for 10 minutes. mMWCNTs-EPI were then held tightly to the flask wall by magnetic forces. The free EPI was aspirated and measured on a Shimadzu SCL-10AVP series HPLC system coupled with ultraviolet detection set at 480 nm and C_{18} analytical column (150×4.6 mm, 5 μm particle size)

(Beckman Coulter). The binary mobile phase was sodium dihydrogen phosphate (68%) and acetonitrile (32%) delivered at 1.0 mL/min. The loading efficiency of EPI was calculated:[22]

$$\frac{\text{Weight of total EPI} - \text{Free EPI}}{\text{Weight of total EPI}} \times 100\%$$

mMWCNTs-EPI were then dispersed in PBS (pH 6) on a shaking table. Every 2 hours, the released solution was collected with external magnets and PBS refreshed (mimicking physiological condition of urine). The EPI release ratio from mMWCNTs-EPI was determined according to the change in concentration. Areas under concentration–time curves for EPI were calculated.

In vivo evaluation of retention

The retention of mMWCNTs-EPI in bladders was determined in 15 female rats with a 3,200 G magnetic field. Rats were killed at 12, 24, 48, 72, and 96 hours after mMWCNTs-EPI instillation (three rats at each time point). Bladders excised at different time points were fixed with 4% paraformaldehyde, embedded in paraffin, and serially sectioned. The 4 μm-thick sections underwent H&E staining.

Quantitative detection of apoptosis in vitro

To measure cell apoptosis, 5637 and T24 cells were seeded onto six-well plates at a density of 10^5 cells/well. Group 1 was the control. Groups 2–4 were treated for 24 hours with a magnetic field and 40 μg/mL mMWCNTs; 2 μg/mL EPI; and a magnetic field and mMWCNTs-EPI (containing 2 μg/mL EPI). The culture medium was refreshed at 2, 4, 6, 8, 10, 12 and 24 hours to mimic urination. Cells were collected and subjected to annexin V–propidium iodide staining using the FITC–annexin V apoptosis-detection kit. Apoptotic cells were analyzed with a FACSDiva Flow Cytometer (BD Biosciences).

Quantitative detection of proliferation in vitro

To examine proliferation of 5637 and T24 cells, cells were seeded onto 24-well plates at a density of 5×10^4 cells/well. The groups were treated as described in (Cell morphology test section) and (Quantitative detection of apoptosis in vitro section). All groups were treated with EdU for 2 hours and then incubated with the Apollo 567 kit. Nuclei were counterstained with DAPI. Images were captured using fluorescence microscopy, and digital histomorphometric analysis was performed with ImageJ software.

Chemically induced bladder cancer model in rats

An MNU-induced rat-bladder tumor model described previously was used, with some modifications.[23] Female Wistar rats were anesthetized with intraperitoneal injections of 3% pentobarbital (30 mg/kg). Then, MNU was instilled intravesically via shortened 3F epidural anesthesia catheters within 45 minutes of preparation after the bladders had been drained. Instillation was performed every other week for a total of four doses (8 weeks).

Antitumor activity in vivo

The 30 rats were divided randomly into five groups. Group 1 was administered as the control. The other groups were induced BC models as previously described. After 8 weeks, groups 2–5 received intravesical instillation with the 0.1 mL PBS, 0.25 mg/0.1 mL mMWCNTs, 0.1 mg/0.1 mL EPI, and 0.1 mL mMWCNTs-EPI (containing 0.1 mg EPI and 0.25 mg mMWCNTs), respectively. They received intravesical instillation on a weekly basis six times. Groups 3 and 5 were maintained in the 3,200 G magnetic field (group 5 treatment is illustrated in Scheme 1, B and C). All rats were killed and subjected to necropsy (one in the mMWCNTs group was killed by an unintended anesthetic overdose). A tumor was defined as a lesion >0.5 mm in diameter.[24] Tumor volume was calculated:

$$V\ (mm^3) = 0.5 \times (\text{length}) \times (\text{width})^2.$$

Immunohistochemistry study

The 4 μm-thick bladder-tissue sections of all groups underwent immunohistochemical staining for BCL2, BAX, cleaved caspase 3, and immunofluorescence staining of Ki67. Negative control sections were incubated without the primary antibody. Digitized images were subsequently analyzed using Image-Pro Plus 6.0, and average optical density (integrated optical density/area) positive reactions used to evaluate the expression of BCL2, BAX, and cleaved caspase 3. The ratio of $Ki67^+$ cells was analyzed with ImageJ software.

Statistical analysis

All statistical analyses were conducted with SPSS 20.0 software. Data are expressed as mean ± SD for continuous variables. Continuous data were compared among the groups via one-way ANOVA. Tukey's test was used to analyze multiple comparisons between groups. Two-tailed $P<0.05$ indicated statistical significance.

Results

Characterization of mMWCNTs

The preparation of mMWCNTs is illustrated in Scheme 1A. Figure 1A and B show transmission electron microscopy and field-emission scanning electron microscopy of prepared mMWCNTs. The length of raw MWCNTs was 10–30 μm, and the length of MWCNTs–COOH cut by mixed acid became 200–1,000 nm. (Figure 1Ai and ii). Close observation revealed that the MWCNTs–COOH were wrapped tightly with nano-Fe_3O_4 on the surface (Figure 1Aiv). mMWCNTs-suspension ζ-potential was –47.31±0.16 mV, which showed good stability in aqueous solution.

FTIR spectra of MWCNTs–COOH and mMWCNTs showed several peaks at 3,434 cm^{-1}, 1,626 cm^{-1}, 1,384 cm^{-1}, and 1,045 cm^{-1} (Figure 1C). These peaks were ascribed to O–H bonds,[25] C=O groups,[26] and C–OH and C–O stretching vibrations,[27] respectively. The peak at 582 cm^{-1} of mMWCNTs (Figure 1Cii) was assigned to metal oxygen.[26] X-ray diffraction confirmed the metal–oxygen bonds in the mMWCNTs (Figure 1D). According to Joint Committee on Powder Diffraction Standards file 190629 for the magnetite, six diffraction peaks of mMWCNTs at 2θ=30.16°, 35.58°, 43.22°, 53.70°, 57.22°, and 62.87° were attributed to the (220, 311, 400, 422, 511) and (440) crystal planes of cubic Fe_3O_4.[28] Furthermore, the main feature of the X-ray-diffraction pattern of CNTs was a graphite-like peak (002).[29] The diffraction peaks of mMWCNTs at 2θ=26.02° was attributed to the (002) peak of CNTs, which is not obvious. This suggested that mMWCNTs were wrapped by Fe_3O_4 NPs.

The magnetic hysteresis curve of mMWCNTs was determined by alternating-gradient magnetometry (Figure 1E). The mMWCNTs showed superparamagnetic behavior, and the maximum saturation magnetization value is 19.13 emu/g. Residual magnetization and coercivity were both zero. The magnetization curve showed an invertible S shape. There was no hysteresis in the sample. Macroscopic magnetic parameters of mMWCNTs were measured via the 1 mg/mL mMWCNTs suspension. When an external magnet was applied, the mMWCNTs separated from the suspension and were rapidly attracted to the magnet to clear the suspensions (Figure 1F). However, the mMWCNTs returned to suspensions after gentle shaking. Only a trace of mMWCNTs sediments was observed after storage for 15 days, indicating excellent aqueous stability.

Toxicity of mMWCNTs

When treated with different concentrations of mMWCNTs, mMWCNTs showed little toxicity against 5637 and T24 cells

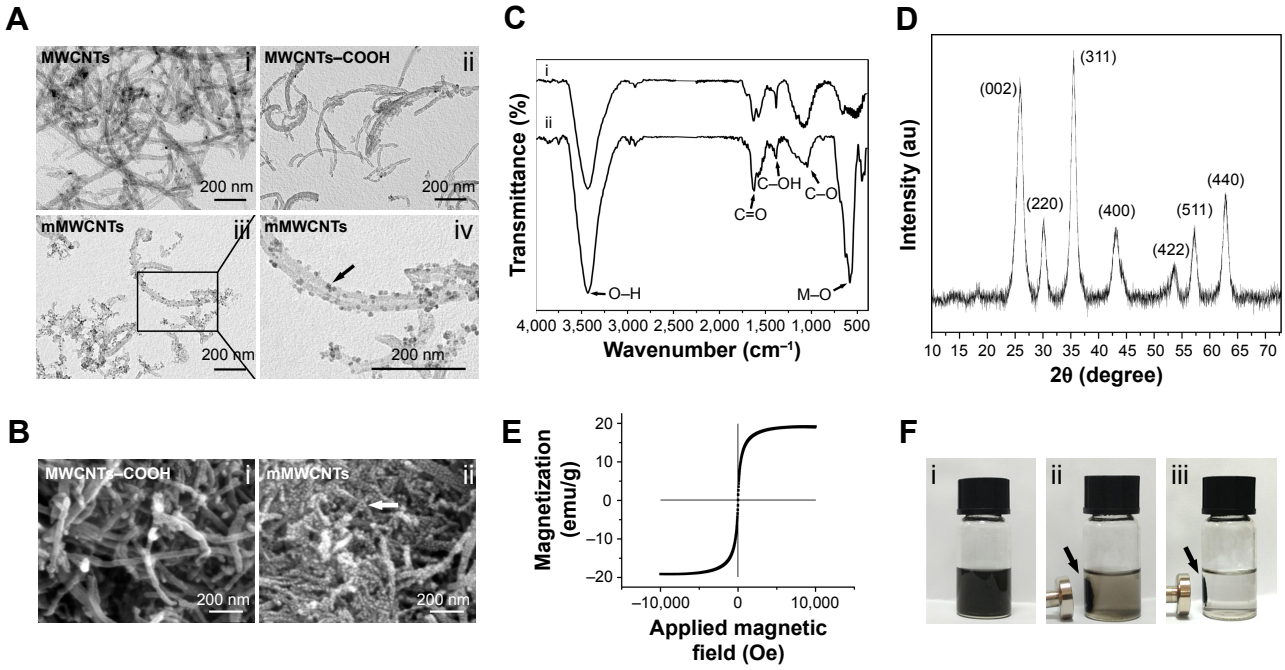

Figure 1 Characterization of MWCNTs, MWCNTs-COOH, and mMWCNTs.

Notes: (**A**) TEM images of MWCNTs, MWCNTs-COOH, and mMWCNTs; black arrow indicates that the MWCNTs-COOH were wrapped tightly with nano-Fe_3O_4 on the surface. (**B**) FESEM images of MWCNTs-COOH and mMWCNTs; white arrow indicates the nano-Fe_3O_4 on the surface of MWCNTs-COOH. (**C**) FTIR spectra of MWCNTs-COOH (i) and mMWCNTs (ii). (**D**) XRD of mMWCNTs. (**E**) Magnetic hysteresis curve of mMWCNTs. (**F**) mMWCNTs dispersed in water without a magnet (i) or with a magnet for 2 minutes (ii) and 5 minutes (iii).

Abbreviations: MWCNTs, multiwalled carbon nanotubes; MWCNTs-COOH, carboxylated MWCNTs; mMWCNTs, magnetic MWCNTs-COOH; TEM, transmission electron microscopy; FESEM, field-emission scanning electron microscopy; FTIR, Fourier-transform infrared spectroscopy; XRD, X-ray diffraction.

(Figure S1). The ratio of EdU-labeled cells was calculated to examine the effect of mMWCNTs on cell proliferation. There was no difference between 40 μg/mL mMWCNTs groups and control groups (Figure 2B and C). F-actin staining was found predominantly in cortical structures around the cell periphery, with a few thin stress fibers located within the cell body. Alignment of F-actin fibers increased in all periods of mitosis (Figure 2A, red arrow). There were no obvious morphological changes or reorganization of F-actin cytoskeleton in either group (Figure 2A).

The toxicity of mMWCNTs in vivo was determined in 12 female rats. During the experiment, there was no mortality or systemic serum biochemical toxicity induced by mMWCNTs (Table S1). Neither mMWCNTs agglomerates nor any visible signs of toxicity (eg, inflammatory cells or histopathological changes) were found in major organs (Figure 2D). There were no abnormal behavioral changes, including diarrhea, vomiting, anorexia, or lethargy.

Sustained EPI release and prolonged retention in rat bladder

The loading procedure for mMWCNTs with EPI solutions resulted in a loading percentage of 40.4%±9.6%. Figure 3A and B shows that the release of EPI from mMWCNTs-EPI was slower, and the decrease in concentration was moderate and lasted longer than free EPI. The sustained release of EPI from mMWCNTs-EPI resulted in the area under the curve nearly tripling (Figure 3C).

mMWCNTs-EPI were stable in rat bladder after 12 hours with external magnets (Figure 3D). The amount of mMWCNTs-EPI and the mMWCNTs-EPI-covered surface areas along the urothelium decreased with time. There were some remnants until 96 hours.

In vitro antitumor activity

mMWCNTs-EPI showed more significant cytotoxicity on 5637 and T24 cells than free EPI when the culture medium

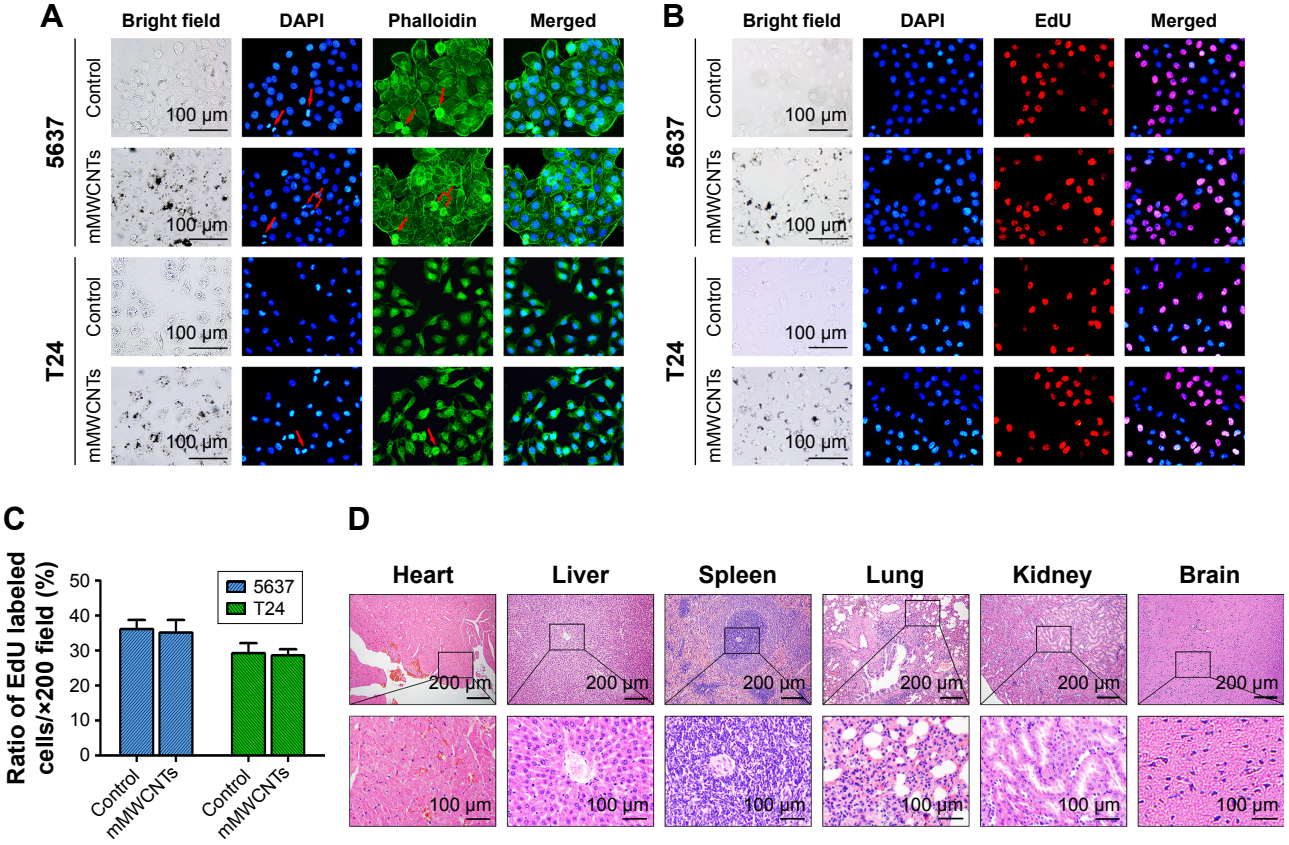

Figure 2 Toxicity of mMWCNTs in vitro and in vivo.

Notes: (**A**) Immunofluorescence-staining microscopy of F-actin cytoskeleton (phalloidin, green) and nuclei (DAPI, blue) of 5637 and T24 cells treated with 40 μg/mL mMWCNTs for 72 hours. Red arrows indicate increased alignment of F-actin fibers over all periods of mitosis. (**B**) Immunofluorescence-staining microscopy of EdU (red) and nuclei (blue) of 5637 and T24 cells treated with 40 μg/mL mMWCNTs for 72 hours. (**C**) Corresponding ratiometric analyses of ratio of EdU-labeled cells. Data presented as mean ± SD. (**D**) H&E-stained rat hearts, livers, spleens, lungs, kidneys, and brains after 2.5 mg/mL mMWCNTs instilled intravesically every 3 days for 1 month.

Abbreviations: mMWCNTs, magnetic multiwalled carbon nanotubes; EdU, ethynyl deoxyuridine.

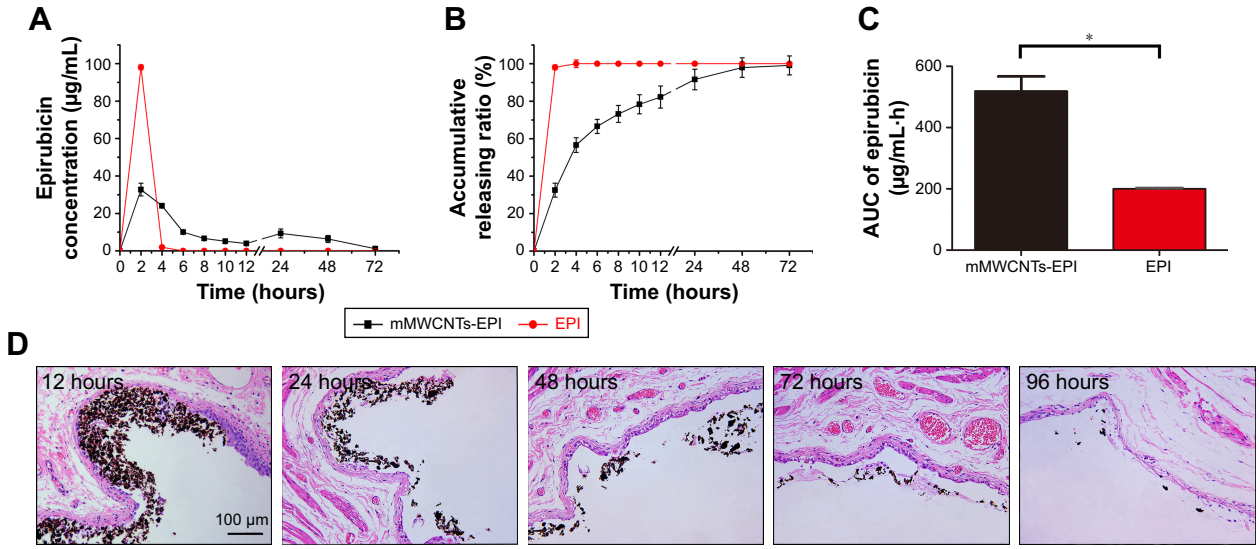

Figure 3 The sustained release of EPI from mMWCNTs-EPI system and prolonged retention in rat bladder.
Notes: (**A**) The EPI release curve of mMWCNTs-EPI and EPI solution. (**B**) The EPI accumulative releasing ratio from mMWCNTs-EPI and EPI solution. (**C**) The areas under the AUC values of EPI. (**D**) The retention of mMWCNTs-EPI system in rat bladder. Exemplary H&E-stained tissue sections from urinary bladders of rats maintained in magnetic field of 3,200 G for 12, 24, 48, 72, and 96 hours after mMWCNTs-EPI instillation. Data presented as mean±SD. *$P<0.05$.
Abbreviations: EPI, epirubicin; mMWCNTs, magnetic multiwalled carbon nanotubes; AUC, area under curve (concentration–time).

was refreshed every 2 hours (Figure S2). Flow-cytometry results demonstrated that the free EPI and mMWCNTs-EPI groups showed higher apoptotic ratios than control and mMWCNTs groups. Versus free EPI, apoptotic ratios in the mMWCNTs-EPI groups increased significantly (Figure 4A and B). Significantly lower ratios of EdU-labeled cells per high-power field (magnification 200×) were observed in mMWCNTs-EPI-treated cells relative to free EPI groups (Figure 5A). Statistical analysis showed that the mMWCNTs-EPI groups demonstrated significantly less proliferation than free EPI groups (Figure 5B).

In vivo antitumor activity

Representative bladder tumors from the five groups are shown in Figure 6A (black arrows). Administration of PBS and mMWCNTs caused no markedly different reduction in the growth of bladder tumors, neither total tumor volume per rat nor volume of each tumor. In terms of efficacy,

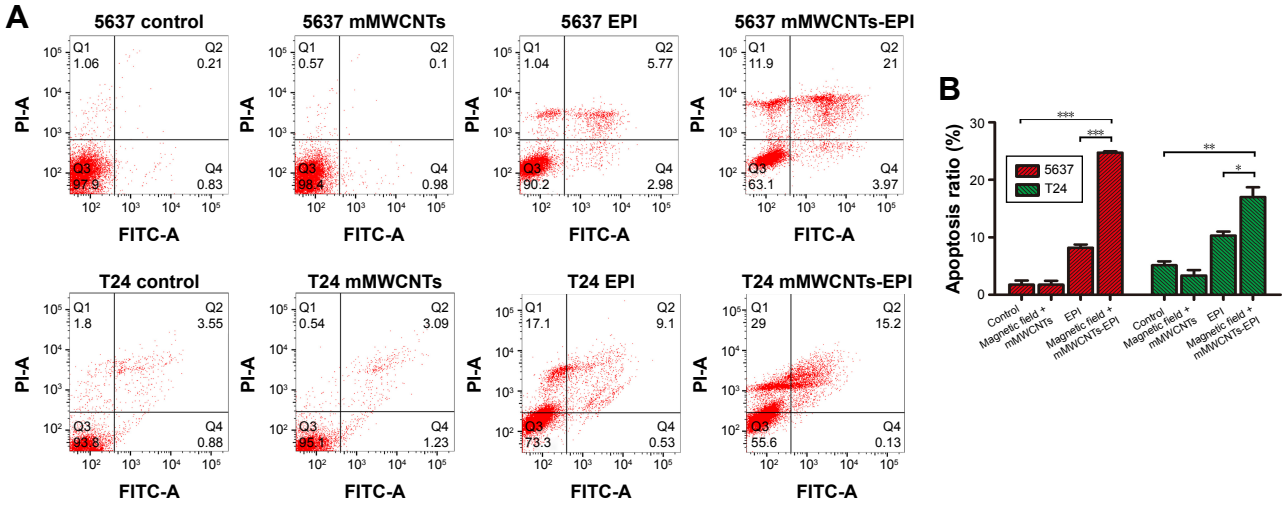

Figure 4 In vitro apoptosis-inducing activity.
Notes: (**A**) Apoptotic cells in groups of 5637 and T24 cells with different treatments. Representative flow-cytometry plots. Q1 represents necrotic cells, Q2 late-apoptosis cells, Q3 living cells, and Q4 early-apoptosis cells. (**B**) Graphic representation of apoptosis rate of each group. Data presented as mean ± SD. *$P<0.05$; **$P<0.01$; ***$P<0.001$.
Abbreviations: FITC, fluorescein isothiocyanate; PI, propidium iodide; mMWCNTs, magnetic multiwalled carbon nanotubes; EPI, epirubicin.

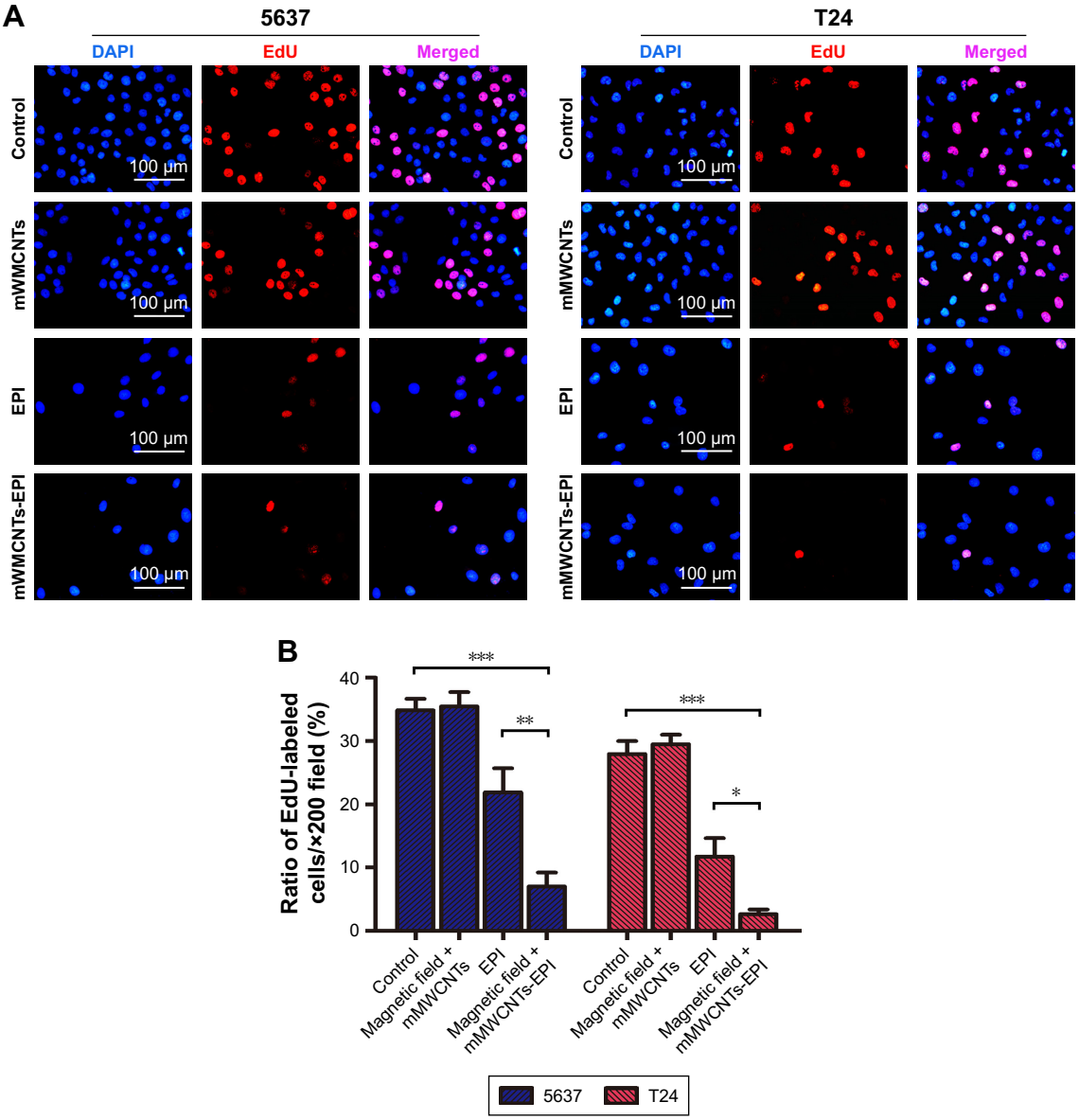

Figure 5 In vitro proliferation-inhibition activity.
Notes: (**A**) Immunofluorescence-staining microscopy of EdU (red) and nuclei (blue) of 5637 and T24 cells treated with 40 μg/mL mMWCNTs and control groups. (**B**) Graphic representation of EdU-labeled cell ratio of each group in A. *$P<0.05$, **$P<0.01$, ***$P<0.001$.
Abbreviations: EdU, ethynyl deoxyuridine; mMWCNTs, magnetic multiwalled carbon nanotubes; EPI, epirubicin.

the mMWCNTs-EPI group achieved better efficacy than free EPI for inhibition of tumor volume (Figure 6B and C). In addition, one unilateral hydronephrosis appeared in both the PBS and mMWCNTs groups, and one bilateral hydronephrosis appeared in the PBS group (Figure 7). Representative images and H&E-stained microscopy of kidney in different groups are shown in Figure 7A and B. Corresponding ratios of hydronephrosis in different groups are displayed in Figure 7C. The hydronephrosis was caused by ureter or vesicoureteric junction invasion.

Enhanced apoptosis and inhibited proliferation by mMWCNTs-EPI

The expression of BAX and cleaved caspase 3 was weak, while BCL2 increased in the PBS and mMWCNTs groups. The EPI and mMWCNTs-EPI groups had contrasting expression patterns compared with the PBS and mMWCNTs groups (Figure 8). The data also showed that the mMWCNTs-EPI group had higher expression of BAX and cleaved caspase 3 and lower expression of BCL2 than the EPI group (Figure 8B).

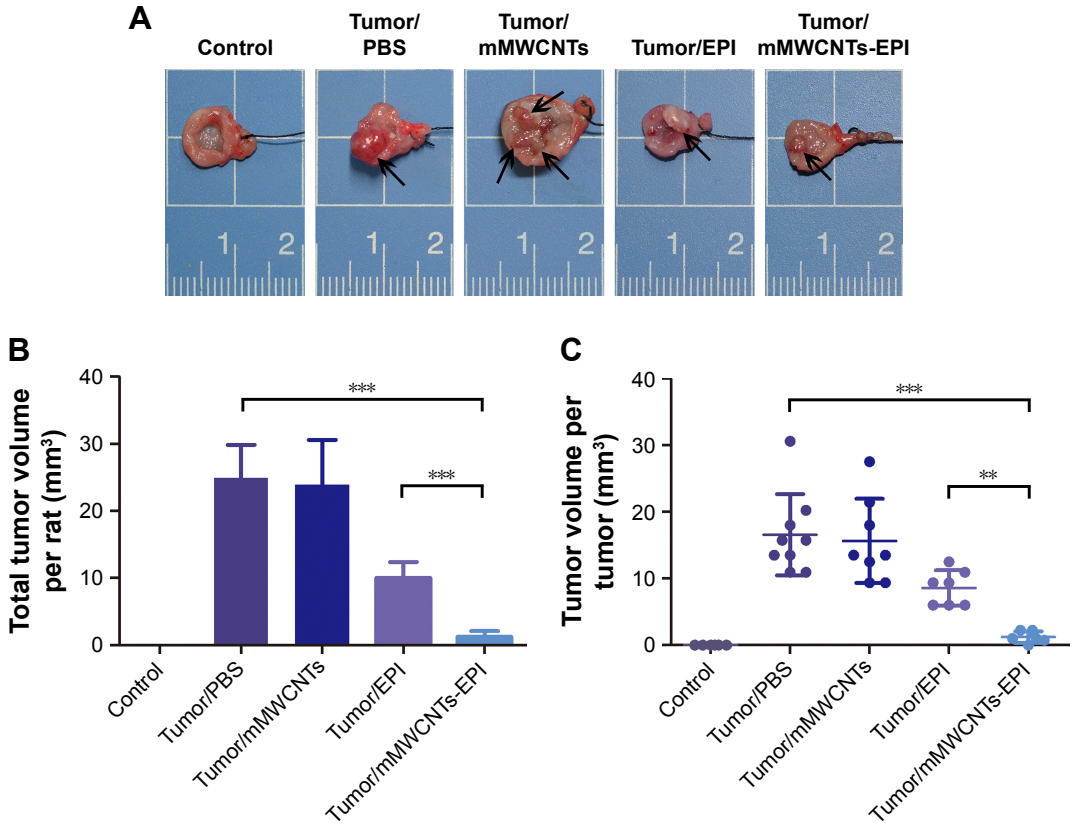

Figure 6 In vivo antitumor activity on bladder cancer.
Notes: (**A**) Representative images of bladder tumors in different groups (black arrow). (**B**) Summary of total tumor volume per rat. Data presented as mean ± SD. (**C**) Graphic representation of the tumor volume. $^{**}P<0.01$; $^{***}P<0.001$.
Abbreviations: mMWCNTs, magnetic multiwalled carbon nanotubes; EPI, epirubicin.

Immunofluorescence-staining results indicated that Ki67$^+$ cells were nearly negative in the control group, but obviously increased in the PBS and mMWCNTs groups (Figure 9). After intravesical instillation therapy with EPI or mMWCNTs-EPI, the ratios of Ki67$^+$ cells decreased significantly. In addition, the mMWCNTs-EPI group showed more inhibition in Ki67 expression than the EPI group (Figure 9).

Discussion

We describe a novel magnetic carboxylated mMWCNTs-based system. This is an excellent delivery system for chemotherapeutic drugs in intravesical instillation. CNTs have been investigated for possible applications in delivering chemotherapy drugs with large surface area.[15,30] Magnetite Fe_3O_4 NPs were introduced to decorate MWCNTs as mMWCNTs. As such, mMWCNTs offered superparamagnetic behavior at room temperature. This superparamagnetic property is very important for the application of magnetic NPs in biomedicine, rather than bulk material. The magnetic NPs showed good magnetic response characteristics via an external magnetic field, and remained monodisperse without an external magnetic field to prevent blocking blood vessels or other lumens.[31]

Studies have shown that chitosan,[13,14] liposomes,[32] and hydrogels[33] are other candidates for local drug delivery. The mMWCNTs-based delivery system has several advantages vs existing systems. First, most drugs in previous delivery systems would be separated from bladder mucosa by the encapsulation barrier or the gel system with a loose cross-linking structure. The drug effect needs to overcome steric hindrance first. However, the mMWCNTs-EPI system is tightly attached to the bladder mucosa. Aggregation of mMWCNTs-EPI under a magnetic field can increase the mucoadhesion of EPI to the tumor. Second, the gel matrix or hydrogel may swell and block the vesicoureteric junction. mMWCNTs solve this issue. mMWCNTs are more clinically convenient and do not lead to vesicoureteric junction blockage. Third, the synthetic steps underlying mMWCNTs are simple and fast. The mMWCNTs mixture was able to be stored at room temperature for a long time, and mMWCNTs-EPI can be

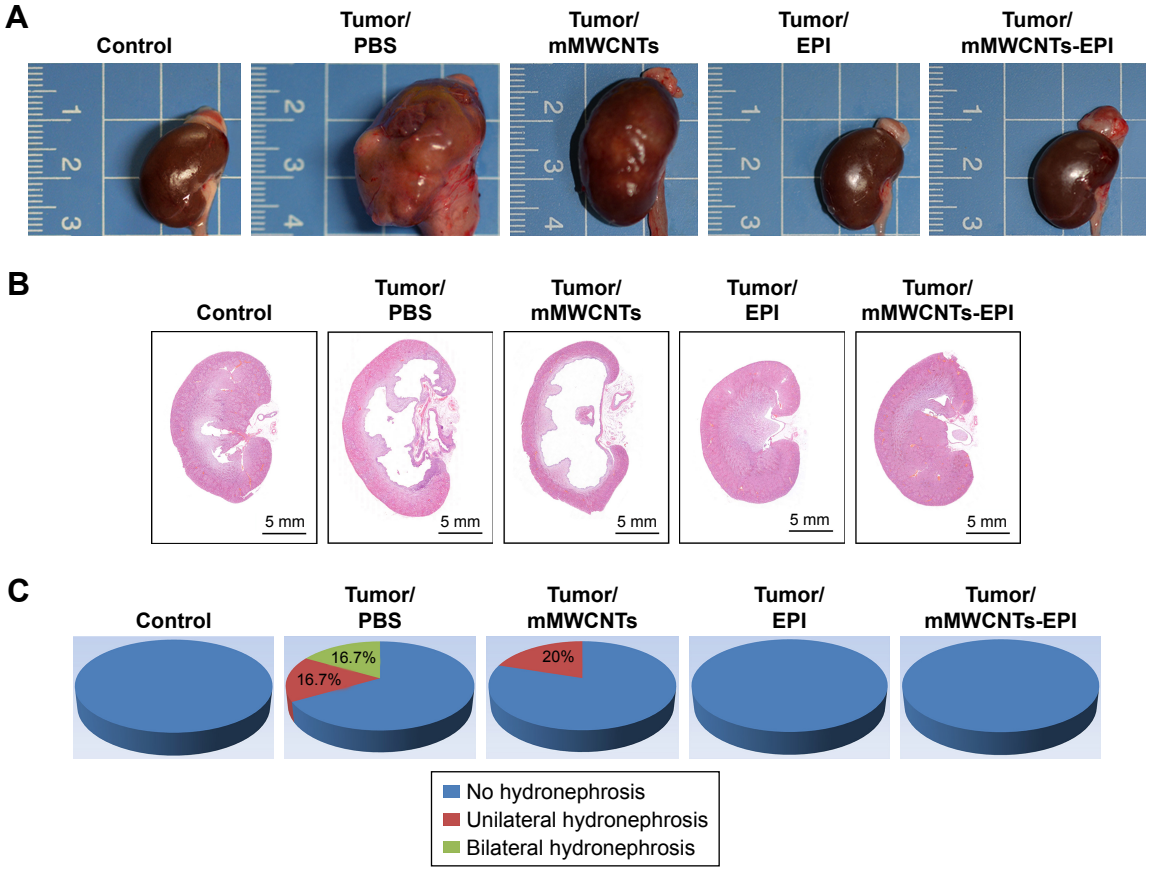

Figure 7 Representative images and H&E-stained sections of kidneys in different groups.
Notes: (**A**) Representative images of kidneys in different groups: normal or hydronephrosis. (**B**) H&E-stained exemplary tissue sections of kidneys in different groups. (**C**) Summary of hydronephrosis in different groups, including unilateral hydronephrosis and bilateral hydronephrosis.
Abbreviations: mMWCNTs, magnetic multiwalled carbon nanotubes; EPI, epirubicin.

readily prepared when needed. Moreover, the mMWCNTs system showed better retention after 96 hours (Figure 3D).

Toxicity, low dispersion, and poor solubility of pristine MWCNTs have limited their biomedical applications.[34] However, research has indicated that highly functionalized and water-dispersible MWCNTs do not accumulate in or injure any tissues.[35] Methods to functionalize MWCNTs include decoration with polyacrylic acid,[41] polysaccharide,[36] alginate sodium,[37] chitosan,[38] and polyethylene glycol.[39] However, our method utilized an acid mixture to carboxylate MWCNTs and reduce their length. This significantly decreased toxicity.[35] Moreover, MWCNTs–COOH were decorated with Fe_3O_4 via coprecipitation of Fe^{2+} and Fe^{3+}, which is a facile option without any assistance from organic solvents.[40]

Traditional NP-based drug-delivery systems will be distributed throughout most tissue after venous injection. However, the wall of the urinary bladder is an effective barrier between the urinary system and blood circulation.[8] In contrast to intravenous injection, intravesical instillation can further minimize the potential toxicity of the mMWCNTs. Figures 2 and S1 show that the mMWCNTs had little cytotoxicity or systemic toxicity. These results suggested that mMWCNTs were safe materials for intravesical instillation.

EPI was periodically released from the mMWCNTs-EPI system with urination cycles (Scheme 1B). In general, the utilization efficiency of EPI through the urothelium is governed by the degree of ionization at bladder pH, time of exposure to tissue, and urinary output frequency.[42] By preventing EPI from being washed away during urine voiding with magnetic fields, exposure of EPI was prolonged and the initial burst release reduced (Figure 3).

Research has indicated that the amount of EPI loaded on MWCNTs–COOH is pH-dependent.[20] The π–π stacking interaction, hydrophobic interaction, and hydrogen-bonding interaction between the EPI–OH and tube-surface–COOH groups lead to three possible interactions between EPI and MWCNTs–COOH.[20] When –OH ionizes to $–O^-$ at a high pH, the electron-donating strength is improved[43] to strengthen the π–π interaction between the EPI and CNTs. This increases adsorption affinity.[44] On the contrary, EPI would release

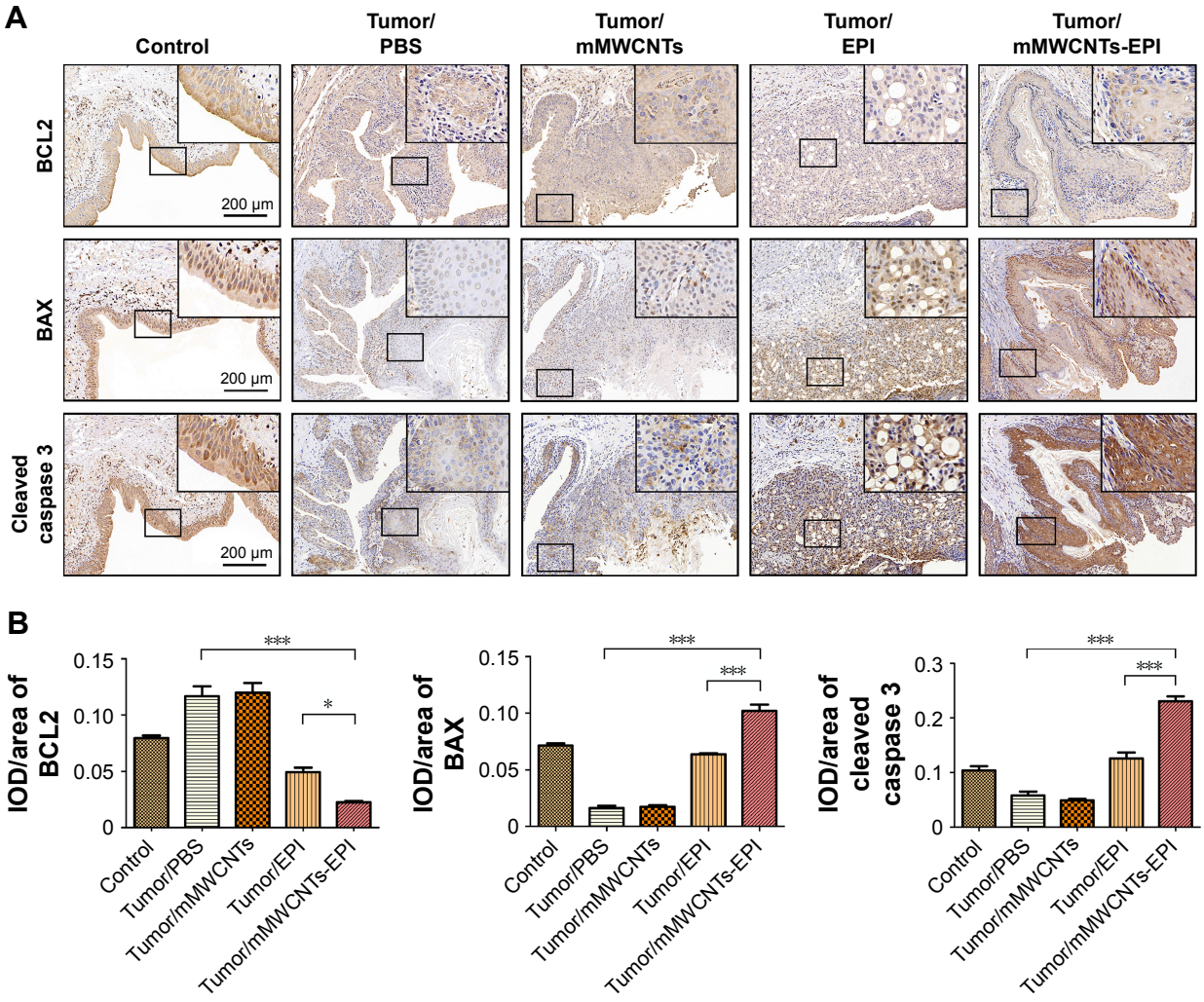

Figure 8 Immunohistochemical staining of exemplary tissue sections of bladders in different groups and statistical analysis of the IOD/area data.
Notes: (**A**) Representative light-microscopy sections of BCL2, BAX, and cleaved caspase 3-stained bladder tissue; (**B**) statistical analysis of IOD/area data of bladder-tissue sections for BCL2, BAX, and cleaved caspase 3. *$P<0.05$, ***$P<0.001$.
Abbreviations: IOD, integrated optical density; mMWCNTs, magnetic multiwalled carbon nanotubes; EPI, epirubicin.

from the mMWCNTs-EPI system at low pH value. Urine is normally slightly acidic.[8] Similar to prior work,[14] we performed our experiments at pH 6. Figure 2A and B shows that EPI had been totally released from the mMWCNTs-EPI system in continuous PBS (pH=6) irrigation after 72 hours. EPI bioavailability via the mMWCNTs-EPI system almost tripled vs free EPI (Figure 3C). Therefore, EPI offered sustained-release behavior for mMWCNTs-EPI in a bladder microenvironment, as expected.

The mMWCNTs-EPI system encouraged antitumor activity both in vitro and in vivo vs traditional intravesical instillation. Figures 4 and 5 confirm that the mMWCNTs-EPI group had better tumor-growth inhibition and induced more apoptosis in vitro than free EPI when given at equivalent doses as free EPI. Figures 6 and 7 indicate that mMWCNTs-EPI are an effective intravesical instillation system for the treatment of BC. EPI acts by interfering with syntheses of DNA, RNA, and protein, as well as cytocidal activity.[45] Caspase 3 is a major executive caspase in mitochondria-dependent apoptosis.[46] Increased BAX and decreased BCL2 expression promote mitochondria-dependent apoptosis.[47] The expression of Ki67 is strongly associated with tumor-cell proliferation.[48,49] Our findings suggested that sustained release of EPI from the mMWCNTs-EPI system promoted mitochondria-dependent apoptosis and inhibited proliferation (Figures 8 and 9).

mMWCNTs increased residence time of EPI in the bladder via an external magnet, but this study does have some limitations. This system could not target the tumor site accurately in rat models, even using external magnets. Some other approaches, such as decorating mMWCNTs with tumor-targeted molecules, could be used. The precise placement of magnets for postoperative care should be a good

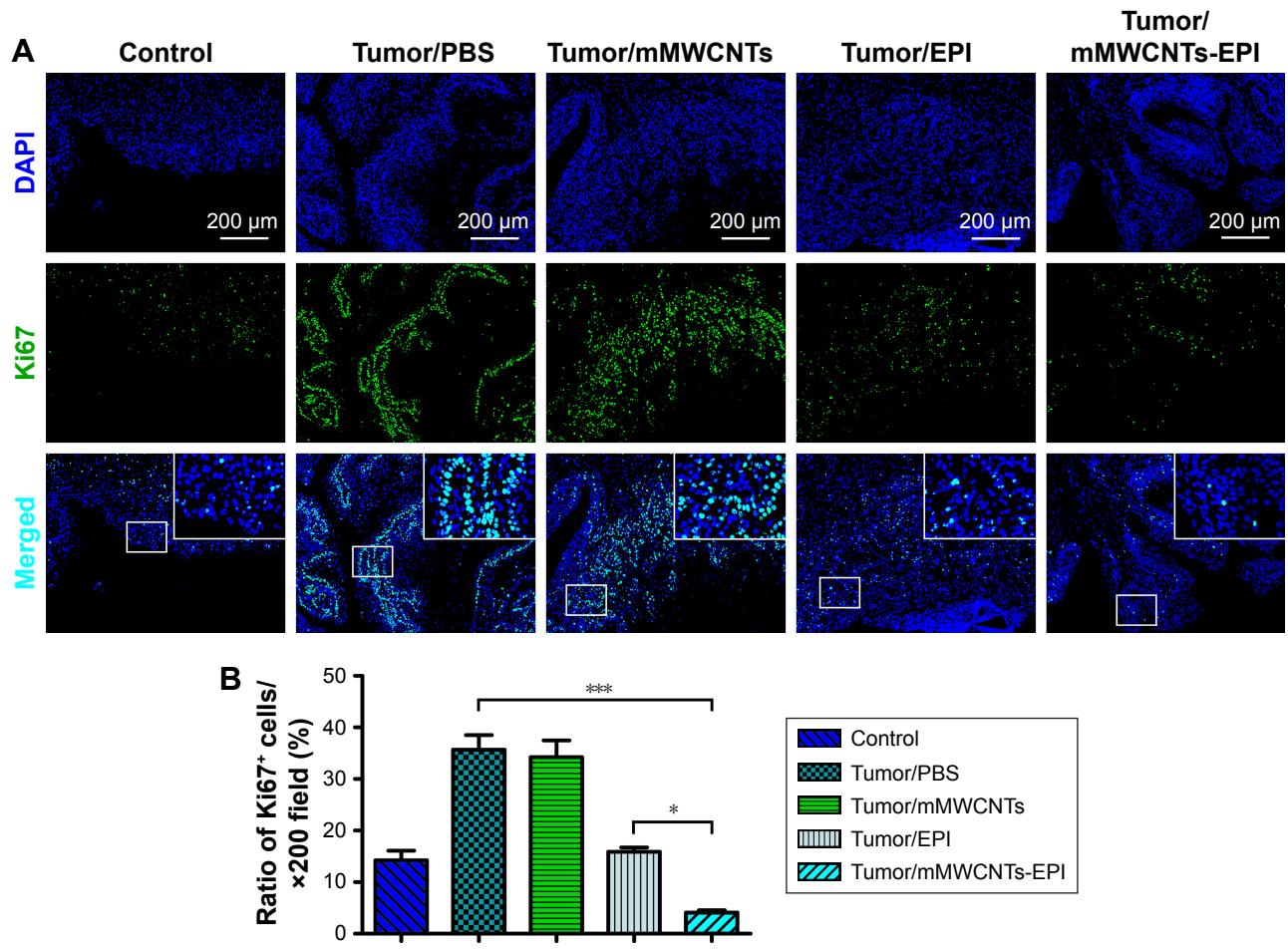

Figure 9 Immunofluorescence-stained exemplary tissue sections of bladders in different groups and statistical analysis of the Ki67$^+$ cells.
Notes: (**A**) Representative light-microscopy sections of Ki67 (green) and nuclei (DAPI, blue) stained bladder tissue; (**B**) statistical analysis of Ki67$^+$ cells of bladder-tissue sections in different groups. *P<0.05, ***P<0.001.
Abbreviations: mMWCNTs, magnetic multiwalled carbon nanotubes; EPI, epirubicin.

way to improve the efficacy of mMWCNTs-EPI in clinical applications. A magnetic belt for the mMWCNTs-EPI system could also be envisioned.

Conclusion

This study successfully developed a safe magnetic adhesion system for the urothelium. The results showed that the mMWCNTs-EPI system effectively extended the duration of EPI in intravesical instillation under external magnets. The mMWCNTs-EPI system enhanced EPI cytotoxicity and inhibited cell proliferation in BC, both in vitro and in vivo. This system can enhance therapeutic effects and decrease side effects of BC by utilizing the synergistic effects of magnetic retention and chemotherapy.

Acknowledgments

This work was supported by the National Natural Science Foundation of China (grant 81572534), Natural Science Foundation of Shandong (grant ZR2016HM32), Shandong Key Research and Development Plan (grants 2015GSF118096, 2017GSF218078, and 2018GSF118189), and the Medical and Health Technology Development Project of Shandong (grant 2016WS0444). We appreciate Professor Lijie Ci, Professor Pengchao Si, Chenglong Dong, and Xiangkun Nie for helpful discussions on the synthesis of mMWCNTs. We would like to thank Professor Jun Li and Shasha Li for HPLC measurements.

Disclosure

The authors report no conflicts of interest in this work.

References

1. Burger M, Catto JW, Dalbagni G, et al. Epidemiology and risk factors of urothelial bladder cancer. *Eur Urol*. 2013;63(2):234–241.
2. Babjuk M, Böhle A, Burger M, et al. EAU guidelines on non-muscle-invasive urothelial carcinoma of the bladder: update 2016. *Eur Urol*. 2017;71(3):447–461.
3. Frantzi M, van Kessel KE, Zwarthoff EC, et al. Development and validation of urine-based peptide biomarker panels for detecting bladder cancer in a multi-center Study. *Clin Cancer Res*. 2016;22(16):4077–4086.

4. Loras A, Trassierra M, Sanjuan-Herráez D, et al. Bladder cancer recurrence surveillance by urine metabolomics analysis. *Sci Rep*. 2018; 8(1):9172.
5. Yeung C, Dinh T, Lee J. The health economics of bladder cancer: an updated review of the published literature. *Pharmacoeconomics*. 2014; 32(11):1093–1104.
6. Ploeg M, Aben KK, Kiemeney LA. The present and future burden of urinary bladder cancer in the world. *World J Urol*. 2009;27(3):289–293.
7. Zuiverloon TC, Theodorescu D. Pharmacogenomic considerations in the treatment of muscle-invasive bladder cancer. *Pharmacogenomics*. 2017;18(12):1167–1178.
8. GuhaSarkar S, Banerjee R. Intravesical drug delivery: challenges, current status, opportunities and novel strategies. *J Control Release*. 2010; 148(2):147–159.
9. Tang H, Guo Y, Peng L, et al. In vivo targeted, responsive, and synergistic cancer Nanotheranostics by magnetic resonance imaging-guided synergistic high-intensity focused ultrasound ablation and chemotherapy. *ACS Appl Mater Interfaces*. 2018;10(18):15428–15441.
10. Mariappan L, Shao Q, Jiang C, et al. Magneto acoustic tomography with short pulsed magnetic field for in-vivo imaging of magnetic iron oxide nanoparticles. *Nanomedicine*. 2016;12(3):689–699.
11. Gambardella A, Bianchi M, Kaciulis S, et al. Magnetic hydroxyapatite coatings as a new tool in medicine: a scanning probe investigation. *Mater Sci Eng C Mater Biol Appl*. 2016;62:444–449.
12. Zhao Y, Zhao X, Cheng Y, Guo X, Yuan W. Iron oxide Nanoparticles-Based vaccine delivery for cancer treatment. *Mol Pharm*. 2018;15(5): 1791–1799.
13. Zhang D, Sun P, Li P, et al. A magnetic chitosan hydrogel for sustained and prolonged delivery of Bacillus Calmette-Guérin in the treatment of bladder cancer. *Biomaterials*. 2013;34(38):10258–10266.
14. Sun X, Sun P, Li B. A new drug delivery system for mitomycin C to improve intravesical instillation. *Mater Design*. 2016;110:849–857.
15. Wong BS, Yoong SL, Jagusiak A, et al. Carbon nanotubes for delivery of small molecule drugs. *Adv Drug Deliv Rev*. 2013;65(15):1964–2015.
16. Iijima S, Ichihashi T. Single-shell carbon nanotubes of 1-nm diameter. *Nature*. 1993;363(6430):603–605.
17. Iijima S. Helical microtubules of graphitic carbon. *Nature*. 1991; 354(6348):56–58.
18. Jia G, Wang H, Yan L, et al. Cytotoxicity of carbon nanomaterials: single-wall nanotube, multi-wall nanotube, and fullerene. *Environ Sci Technol*. 2005;39(5):1378–1383.
19. Allegri M, Perivoliotis DK, Bianchi MG, et al. Toxicity determinants of multi-walled carbon nanotubes: the relationship between functionalization and agglomeration. *Toxicol Rep*. 2016;3:230–243.
20. Chen Z, Pierre D, He H, et al. Adsorption behavior of epirubicin hydrochloride on carboxylated carbon nanotubes. *Int J Pharm*. 2011;405(1–2): 153–161.
21. Bellucci S, Chiaretti M, Onorato P, et al. Micro-Raman study of the role of sterilization on carbon nanotubes for biomedical applications. *Nanomedicine (Lond)*. 2010;5(2):209–215.
22. Singh R, Mehra NK, Jain V, Jain NK. Gemcitabine-loaded smart carbon nanotubes for effective targeting to cancer cells. *J Drug Target*. 2013; 21(6):581–592.
23. Steinberg GD, Brendler CB, Ichikawa T, Squire RA, Isaacs JT. Characterization of an N-methyl-N-nitrosourea-induced autochthonous rat bladder cancer model. *Cancer Res*. 1990;50(20):6668–6674.
24. Parada B, Reis F, Figueiredo A, et al. Inhibition of bladder tumour growth by sirolimus in an experimental carcinogenesis model. *BJU Int*. 2011;107(1):135–143.
25. Suo H, Xu L, Xu C. Enhancement of catalytic performance of porcine pancreatic lipase immobilized on functional ionic liquid modified Fe3O4-Chitosan nanocomposites. *Int J Biol Macromol*. 2018;119:624–632.
26. Ahmadian-Fard-Fini S, Salavati-Niasari M, Ghanbari D. Hydrothermal green synthesis of magnetic Fe3O4-carbon dots by lemon and grape fruit extracts and as a photoluminescence sensor for detecting of E. coli bacteria. *Spectrochim Acta A Mol Biomol Spectrosc*. 2018;203:481–493.
27. Mohamed MM, Khairy M, Ibrahem A. Dispersed Ag_2O/Ag on CNT-Graphene composite: an implication for magnificent photoreduction and energy storage applications. *Front Chem*. 2018;6:250.
28. Fan X, Jiao G, Zhao W, Jin P, Li X. Magnetic Fe3O4-graphene composites as targeted drug nanocarriers for pH-activated release. *Nanoscale*. 2013;5(3):1143–1152.
29. Belin T, Epron F. Characterization methods of carbon nanotubes: a review. *Mater Sci Eng B*. 2005;119(2):105–118.
30. Bhirde AA, Patel V, Gavard J, et al. Targeted killing of cancer cells in vivo and in vitro with EGF-directed carbon nanotube-based drug delivery. *ACS Nano*. 2009;3(2):307–316.
31. Mehta RV. Synthesis of magnetic nanoparticles and their dispersions with special reference to applications in biomedicine and biotechnology. *Mater Sci Eng C Mater Biol Appl*. 2017;79:901–916.
32. Kaldybekov DB, Tonglairoum P, Opanasopit P, Khutoryanskiy VV. Mucoadhesive maleimide-functionalised liposomes for drug delivery to urinary bladder. *Eur J Pharm Sci*. 2018;111:83–90.
33. Kolawole OM, Lau WM, Mostafid H, Khutoryanskiy VV. Advances in intravesical drug delivery systems to treat bladder cancer. *Int J Pharm*. 2017;532(1):105–117.
34. Mamidi N, Leija HM, Diabb JM, et al. Cytotoxicity evaluation of unfunctionalized multiwall carbon nanotubes-ultrahigh molecular weight polyethylene nanocomposites. *J Biomed Mater Res A*. 2017;105(11): 3042–3049.
35. Lacerda L, Ali-Boucetta H, Herrero MA, et al. Tissue histology and physiology following intravenous administration of different types of functionalized multiwalled carbon nanotubes. *Nanomedicine (Lond)*. 2008;3(2):149–161.
36. Liu Y, Chipot C, Shao X, Cai W. Edge effects control helical wrapping of carbon nanotubes by polysaccharides. *Nanoscale*. 2012;4(8):2584–2589.
37. Karkeh-Abadi F, Saber-Samandari S, Saber-Samandari S. The impact of functionalized CNT in the network of sodium alginate-based nanocomposite beads on the removal of Co(II) ions from aqueous solutions. *J Hazard Mater*. 2016;312:224–233.
38. Karnati KR, Wang Y. Understanding the co-loading and releasing of doxorubicin and paclitaxel using chitosan functionalized single-walled carbon nanotubes by molecular dynamics simulations. *Phys Chem Chem Phys*. 2018;20(14):9389–9400.
39. Sobhani Z, Behnam MA, Emami F, Dehghanian A, Jamhiri I. Photothermal therapy of melanoma tumor using multiwalled carbon nanotubes. *Int J Nanomedicine*. 2017;12:4509–4517.
40. Lu AH, Salabas EL, Schüth F. Magnetic nanoparticles: synthesis, protection, functionalization, and application. *Angew Chem Int Ed.* 2007; 46(8):1222–1244.
41. Yang F, Jin C, Yang D, et al. Magnetic functionalised carbon nanotubes as drug vehicles for cancer lymph node metastasis treatment. *Eur J Cancer*. 2011;47(12):1873–1882.
42. Giannantoni A, Di Stasi SM, Chancellor MB, Costantini E, Porena M. New frontiers in intravesical therapies and drug delivery. *Eur Urol*. 2006; 50(6):1183–1193; discussion 1193.
43. Chen W, Duan L, Wang L, Zhu D. Adsorption of hydroxyl- and amino-substituted aromatics to carbon nanotubes. *Environ Sci Technol*. 2008;42(18):6862–6868.
44. Lin D, Xingt B. Adsorption of phenolic compounds by carbon nanotubes: role of aromaticity and substitution of hydroxyl groups. *Environ Sci Technol*. 2008;42(19):7254–7259.
45. Khasraw M, Bell R, Dang C. Epirubicin: is it like doxorubicin in breast cancer? A clinical review. *Breast*. 2012;21(2):142–149.
46. Porter AG, Jänicke RU. Emerging roles of caspase-3 in apoptosis. *Cell Death Differ*. 1999;6(2):99–104.
47. Danial NN, Korsmeyer SJ. Cell death. *Cell*. 2004;116(2):205–219.
48. Yang C, Zhang J, Ding M, et al. Ki67 targeted strategies for cancer therapy. *Clin Transl Oncol*. 2018;20(5):570–575.
49. Li LT, Jiang G, Chen Q, Zheng JN. Ki67 is a promising molecular target in the diagnosis of cancer (review). *Mol Med Rep*. 2015;11(3): 1566–1572.

Supplementary materials

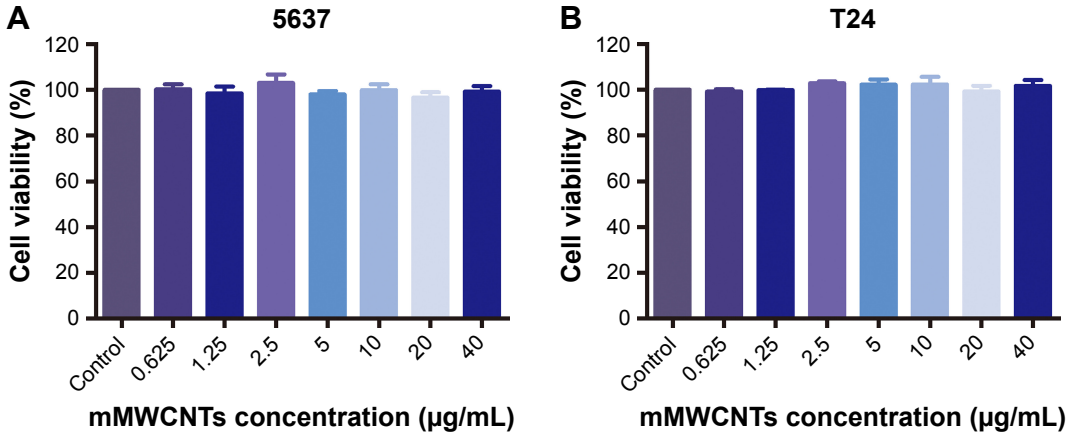

Figure S1 The CCK-8 results of 5637 (**A**) and T24 (**B**) cells treated with 0, 0.625, 1.25, 2.5, 5, 10, 20 and 40 μg/mL mMWCNTs for 72 h.
Abbreviation: mMWCNTs, magnetic multiwalled carbon nanotubes.

Table S1 Serum biochemical analysis between treated group (2.5 mg/L mL mMWCNTs instilled intravesically every 3 days for 1 month) and control group

	ALT (U/L)	AST (U/L)	Scr (μmol/L)	BUN (mg/dL)
Control	35.67±6.73	68.23±15.08	38.51±6.12	15.02±3.37
mMWCNTs	33.32±3.95	67.43±9.01	41.05±7.88	18.03±5.66

Notes: All groups n=6, values mean ± SD. There were no statistically significant differences between groups ($P>0.05$).
Abbreviations: mMWCNTs, magnetic multiwalled carbon nanotubes; ALT, alanine aminotransferase; AST, aspartate aminotransferase; Scr, serum creatinine; BUN, blood urea nitrogen.

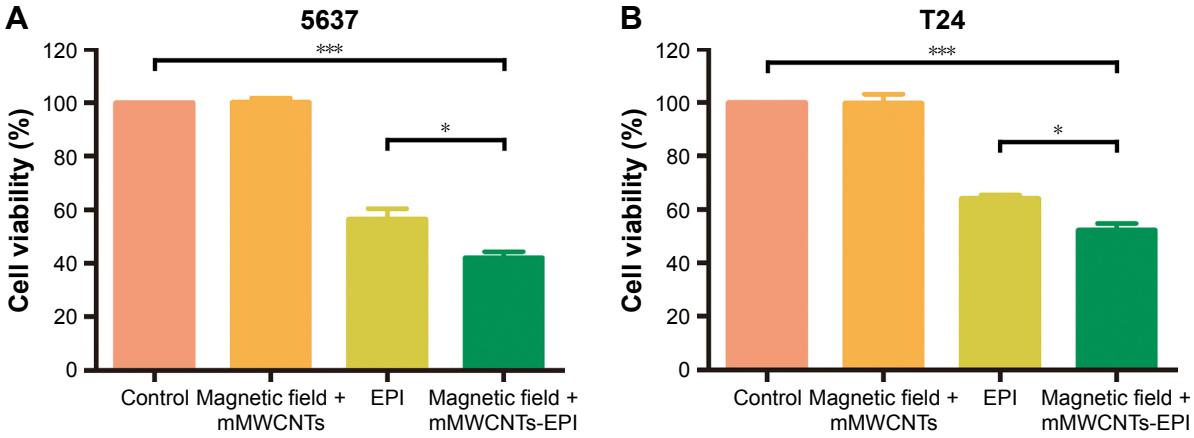

Figure S2 CCK8 results of 5637 (**A**) and T24 (**B**) cells with different treatments.
Note: *$P<0.05$, ***$P<0.001$.
Abbreviations: mMWCNTs, magnetic multiwalled carbon nanotubes; EPI, epirubicin.